arXiv:1703.03416v1 [hep-ph] 9 Mar 2017

# Majoron dark matter from a spontaneous inverse seesaw model

**N. Rojas**[1], **R. A. Lineros**[1], **F. Gonzalez-Canales**[2].

[1] Instituto de Física Corpuscular – CSIC/U. Valencia,
Parc Científic, calle Catedrático José Beltrán 2, E-46980 Paterna, Spain
[2] Fac. de Cs. de la Electrónica, Benemérita Universidad Autónoma de Puebla, Apdo. Postal 542, Puebla, Pue. 72000, México.

**Abstract.** The generation of neutrino masses by inverse seesaw mechanisms has advantages over other seesaw models because the possible new particles of the former can be detected at the TeV scale. We propose a model that generates the inverse seesaw mechanism via spontaneous breaking of the lepton number. In the minimal realization, we extend the Standard Model (SM) with two scalars and two fermions, both groups carrying lepton number but being singlets under the SM gauge group. Moreover, the scalar sector allows spontaneously broken CP symmetry as result of the lepton charge assignment. The model gives rise to two pseudoscalar particles: a massless and a massive Majorons, which correspond to the goldstone boson of the lepton number breaking and a massive pseudoscalar respectively. The latter can take the role of dark matter with main decay channels to neutrinos and massless Majorons. In this scenario, we examine the model phenomenology under the light of the dark matter lifetime. We found that the decay mode to neutrinos is sensitive to $\omega$, which is the ratio between the vevs of the new scalars. We found that the decay mode vanishes completely when $\omega \simeq \sqrt{2/3}$. The decay width to scalars is crucial because it can destabilize drastically the dark matter. However, we found that this width vanishes completely in a certain region of the parameter space. Besides, we suggest a modification to the model solving the scalar decay problem. Finally, we propose a set of mechanisms that explain the Majoron dark matter relic abundance.

PACS numbers: 14.60.Lm, 14.60.St, 14.60.Pq, 95.35.+d, 11.30.Qc

*Keywords:* neutrino masses, dark matter, majoron

## 1. Introduction

The success of the Standard Model of particle physics (SM) has been established thanks to accurate predictions of many experimental observations [1, 2, 3, 4, 5, 6]. Nevertheless, the SM presents some theoretical and experimental issues that it cannot describe. One of these is the Dark Matter (DM), which is the largest matter component ($\sim 85\%$) present in the Universe [7, 8, 9]. Another one is the neutrino oscillations [10, 11, 12, 13], which are a consequence of the still-not-measured neutrino masses. Both issues provide a tantalizing connection between DM and neutrinos that can be realized in many ways (see, for instance, [14, 15]).

From the observations in neutrino oscillation experiments, we get two important features of neutrinos: *i*) the leptonic mixing angles have very large values when compared with the ones in the hadronic sector, *ii*) the neutrino mass scale is very small with respect to the masses of the rest of the SM fermions [16, 17, 18, 19]. These two features could be interpreted as an indication of new physics beyond the SM scale.

The simplest SM-like framework with massive neutrinos assumes that neutrinos are Majorana particles. In this framework, Majorana masses arises via the dimension-5 Weinberg operator [20]. This operator respects main SM symmetries like Lorentz and the $SU(3) \times SU(2) \times U(1)$ gauge structure, and it is build exclusively with SM fields. This operator can be generated at tree level only by minimally extending the SM in three ways. These are renormalizable constructions that are known as type I [21, 22], II [23, 24], and III [25] seesaw mechanisms. Each seesaw construction provides different predictions that can be tested in current and future experiments. The inclusion of new particles is unavoidable in these constructions and the explanation for the neutrino mass scale is closely related to the mass scale for the new particles.

Although in the SM, baryon and lepton numbers are accidental global symmetries, the seesaw mechanism explicits the breaking of lepton number through of the presence Majorana neutrino masses. This issue, in turn, comes from the fact that lepton number is already not a symmetry at the new particle scale. One way to alleviate this is assuming that lepton number is preserved at higher scale but it is spontaneously broken at some intermediate scale. In this scheme, the goldstone boson of the lepton number breaking appears and it is historically know as *The Majoron* [26].

Although the Majoron appears as a massless particle, there are conjectures saying that global symmetries must be broken due to Planck scale effects. This would explain how the Majoron get its small mass [27] and why fully stable DM might not be possible [28]. When the Majoron becomes massive, the most important decay channel for this particle is through neutrinos [23, 29, 30, 31, 32]. For sub-keV majorons, those particles have lifetimes larger than the age of the Universe [29, 31]. A massive Majoron is electrically neutral and might have weak interactions, something that turns it into a potentially suitable Dark matter candidate. However, it is still not well understood how it acquires mass and how to produce a feasible relic DM abundance of massive Majorons in the early Universe. At this point, we could argue that the *goldstone* Majoron and the

Majoron DM are different particles with a common origin.

On top of that, within the type I and III seesaw mechanisms and in order to give rise to small neutrino masses, the mass scale at which the new physics lives is around $10^{12}$ GeV. However, the inclusion of extra fermions singlets, and interactions among themselves and the SM lepton doublet, can show variations of the seesaw mechanism in which the mass scales for the new particles is not necessarily large. In the literature, those variations are called as *low scale seesaw* [33, 34, 35], and our focus will be on the *inverse seesaw mechanism* [34, 36].

In this work we propose a mechanism in which neutrino physics and a Majoron DM candidate are joined together. We use this setting as a scheme based of the inverse seesaw mechanism which is in turn spontaneously generated. The spontaneous symmetry breaking gives rise to a goldstone Majoron and a massive Majoron which is our DM candidate. We describe the basics of the inverse sessaw and our model in Section 2. The implications of our model for the Majoron DM are shown in Sections 3 and 4. Finally, the conclusions are in Section 5.

## 2. The spontaneous inverse seesaw model

As it was advanced, throughout the work we will focus on the inverse seesaw mechanism for neutrino mass generation [34]. In particular, during this section, we will embed this model in a scheme where it is spontaneously generated (although efforts in this way have been presented before, see for instance [37]). On top of that, throughout this section the particle content of the model and its interactions will be described.

### *2.1. The inverse Seesaw*

Among the different schemes for neutrino mass mechanism, the inverse seesaw scenario is characterized by 2 mass scales, which are associated to 2 new fermion singlets per active neutrino species added to the neutrino sector [36]. These new singlets give rise to heavy neutrinos with masses above the TeV scale. This scenario is adequate to be tested with current or near-future planned experiments.

The mass lagrangian for the inverse seesaw can be written as [36, 38]:

$$\mathcal{L} = -\frac{1}{2} n_L^T C \mathcal{M} n_L + h.c.\,, \tag{1}$$

where $n_L^T = (\nu_L, N_1^c, N_2)$ is composed by the SM neutrino $\nu_L$ and the new singlet fermions $N_{1,2}$, then the mass matrix $\mathcal{M}$ is

$$\mathcal{M} = \begin{pmatrix} 0 & m_D & 0 \\ m_D^T & 0 & M \\ 0 & M^T & \mu \end{pmatrix}. \tag{2}$$

The blocks $M$ and $\mu$ characterize the inverse seesaw and $m_D$ is the Dirac block.

This matrix can be perturbatively diagonalized in a similar way to the type-I seesaw when $\mu \ll m_D \ll M$. Even though in the present work we are not going to explore neutrino physics, without loosing generality, we will consider 1 active neutrino and 2 singlets. This framework will provide just one massive light neutrino. Under this setup, the masses of this sector at leading order are:

$$m_\nu = \left(\frac{m_D}{M}\right)^2 \mu, \tag{3}$$

$$m_{\mathcal{N}} = M - \frac{m_D^2}{M} - \frac{\mu}{2}, \tag{4}$$

$$m_{\mathcal{N}'} = M - \frac{m_D^2}{M} + \frac{\mu}{2}. \tag{5}$$

For active neutrino mass of $m_\nu \sim$0.1 eV, heavy neutrinos with masses of $M \sim$100 TeV, and a dirac term of $m_D \sim$10 GeV, we require a $\mu$ parameter to be around 10 MeV [38], which matches our requirement $\mu \ll m_D \ll M$. In this regime, the neutral fermions mixing matrix is

$$U = \begin{pmatrix} 1 & 0 & m_D/M \\ -m_D/\sqrt{2}M & 1/\sqrt{2} & 1/\sqrt{2} \\ -im_D/\sqrt{2}M & -i/\sqrt{2} & i/\sqrt{2} \end{pmatrix}, \tag{6}$$

where the mass eigenstates are given by $(\nu, \mathcal{N}, \mathcal{N}') = (U\, n_L)^T$ and the mass matrix $\mathcal{M}$ is diagonalized by $m_\nu^{diag} = U\mathcal{M}U^T$.

### *2.2. The spontaneous inverse seesaw*

The mass parameters in the inverse seesaw can be generated by means of spontaneous symmetry breaking (SSB) of a global $U_l(1)$ symmetry associated to the lepton number (see, for instance [37, 39]). Our approach uses the following lagrangian:

$$\mathcal{L} = -y_L \bar{L} H N_1^c - y_S S^\dagger \overline{N_2} N_1^c - \frac{y_X}{2} X^\dagger \overline{N_2^c} N_2 + h.c.\,, \tag{7}$$

where $y_i$ are yukawa couplings that after SSB give rise to Eq. 1. The Higgs doublet is defined by $H^T = \left(\chi^+, (v_h + \sigma_h + i\chi_h)/\sqrt{2}\right)$ where $\sigma_h(\chi_h)$ is the (pseudo)scalar component of the Higgs doublet whose vev is $v_h \simeq 246$ GeV, while $\chi^+$ is its charged component.

We have included 2 complex scalar $S$ and $X$ charged with lepton number, but both singlets under $SU(2)_L$ and with zero hypercharge. After the SSB, these fields acquire non-zero vevs, and thus, the mass parameters of the inverse seesaw are defined by:

$$m_D = \frac{y_L v_h}{\sqrt{2}}\,,\; M = \frac{y_S v_S}{\sqrt{2}}\,, \text{and } \mu = \frac{y_X v_X}{\sqrt{2}}\,. \tag{8}$$

By fixing the values of $M$ and $\mu$ and since the yukawa couplings cannot exceed the perturbative limit of $\sqrt{4\pi}$, we obtain lower bounds for $v_S$ and $v_X$:

$$v_S > \frac{M}{\sqrt{2\pi}}\,, \tag{9}$$

$$v_X > \frac{\mu}{\sqrt{2\pi}}\,, \tag{10}$$

| | $L$ | $N_1$ | $N_2$ | $S$ | $X$ |
|---|---|---|---|---|---|
| $SU(2)_L$ | 2 | 1 | 1 | 1 | 1 |
| $U(1)_Y$ | 1/2 | 0 | 0 | 0 | 0 |
| $U(1)_l$ | 1 | $-1$ | $x$ | $1-x$ | $2x$ |

Table 1: Charge assignment of the model.

which can be translated to $v_S > 50$ TeV and $v_X > 5$ MeV for the values previously selected of $M$ and $\mu$. On the contrary, the value of $m_D$ is completely fixed by $y_L$ since $v_h$ has a determined value.

The $U(1)_l$ charges have been assigned by requiring Eq. 7 to be lepton number invariant, and they are shown at Table 1. Note that not all the charges can be fixed by Eq. 7, which leaves the assignations of the fields $N_2$, $S$ and $X$ completely free as a function of the lepton number of $N_2$, which is called $x$. This value can be restricted depending on the scalar potential, an issue depicted in the following subsection.

### *2.3. Scalar potential*

The scalar potential for the new singlets $S$ and $X$ is given by

$$V_{SX} = -\mu_S^2 |S|^2 + \frac{\lambda_S}{4} |S|^4 - \mu_X^2 |X|^2 + \frac{\lambda_X}{4} |X|^4 + \lambda_5 |S|^2 |X|^2 + V_{\rm I}\,, \quad (11)$$

where $\mu_i^2$ are positive mass terms, $\lambda_i$ are adimensional couplings allowed by perturbative limit, and $V_I$ is an $S - X$ interaction term given by:

$$V_{\rm I} = \lambda_{\rm cp} e^{i\delta} X S^{\dagger 3} + \text{h.c.}\,, \quad (12)$$

where $\delta$ is a CP-phase for the coupling $\lambda_{\rm cp}$ which is positive‡.

The addition of $V_I$ fixes the lepton number of the new fields as a function of $x$. For this particular case, the charge assignations are $L_{N_1} = 1$, $L_{N_2} = x = 3/5$, $L_X = 2x = 6/5$, and $L_S = 1 - x = 2/5$, where we have demanded that $X^m S^{\dagger n}$ is dimension 4. We can also take $V_I$ with lower mass dimension in order to keep renormalizability, and thus producing different values of $x$ (see Appendix A).

After SSB, the fields $S$ and $X$ can be written as:

$$S = \frac{1}{\sqrt{2}} \left( v_S e^{i\theta} + \sigma_S + i\chi_S \right) \quad (13)$$

$$X = \frac{1}{\sqrt{2}} \left( v_X e^{i\tau} + \sigma_X + i\chi_X \right)\,, \quad (14)$$

where $\theta$ and $\tau$ are CP-phases. These complex phases in the vev are indicating spontaneous violation of CP. Moreover, considering the role of $\delta$ at 12, we have two

‡ Different models with a similar underlying idea can be found at [29, 40, 41, 30]

sources of CP-violation in this model, whose consequence is allowing the mixing scalar/pseudoscalar [42].

The remaining terms that include the Higgs part are:

$$V_{\rm HSX} = -\mu_H^2 H^\dagger H + \frac{\lambda_H}{4}(H^\dagger H)^2 + \lambda_{HS}\,|S|^2\,H^\dagger H + \lambda_{HX}\,|X|^2\,H^\dagger H\,, \quad (15)$$

where $\mu_H^2$ and $\lambda_H$ are the higgs mass parameter and its quartic self-interaction, while $\lambda_{HS}$ and $\lambda_{HX}$ are the couplings between $H$ and the new scalars.

The full scalar potential is the sum of Eqs. 11 and 15,

$$V_{\rm scalar} = V_{SX} + V_{HSX}\,. \quad (16)$$

The physical fields are extracted after the minimization of the $V_{\rm scalar}$ and plugging back into the Lagrangian the solution of the tadpole equations:

$$\left.\frac{\partial V_{\rm scalar}}{\partial s_0^i}\right|_{s_0^{j\neq i}=0} = 0\,, \quad (17)$$

where $s^{0T} = (\sigma_S, \sigma_X, \sigma_h, \chi_S, \chi_X)$, i.e. it represents all the neutral scalar and pseudoscalar fields of the model but the field $\chi_h$. Afterwards, we still need to write and diagonalize the mass matrices in order to get the physical fields.

Regarding the tadpole equations for $\chi^+$ and $\chi_h$, they are trivially satisfied and do not add relevant information in our context. On the other hand, the minimization conditions 17 give rise to the following relations among the parameters:

$$\tau = 3\theta - \delta - \pi\,, \quad (18)$$

$$\mu_S^2 = \frac{v_S^2}{4}\left(2\epsilon^2\lambda_{HS} + \lambda_S - 6\lambda_{\rm cp}\omega + 2\lambda_5\omega^2\right)\,, \quad (19)$$

$$\mu_X^2 = \frac{v_S^2}{4}\left(2\epsilon^2\lambda_{HX} - 2\lambda_{\rm cp}\,\omega^{-1} + 2\lambda_5 + \lambda_X\omega^2\right)\,, \quad (20)$$

$$\mu_H^2 = \frac{v_S^2}{4}\left(\epsilon^2\lambda_H + 2\lambda_{HS} + 2\lambda_{HX}\omega^2\right)\,, \quad (21)$$

where $\omega = v_X/v_S$ and $\epsilon = v_h/v_S$ which can be as small as $5\times10^{-3}$. The first condition implies that all CP-phases are aligned and therefore some level of CP violation must be present.

### *2.4. Mass spectrum*

The mass matrix for the scalar and pseudoscalar fields is obtained from

$$\frac{\partial^2 V_{\rm scalar}}{\partial s_i^0 \partial s_j^0} \equiv \left\{M^2\right\}_{ij}\,. \quad (22)$$

Recall that we ignore the $\chi^{+,h}$ fields since they are completely decoupled from the rest of scalars, and thus they correspond to the electroweak goldstone bosons.

The CP-phases just mix up the scalar and pseudoscalar sectors inside $M^2$. However, one can transform the mass matrix in such a way that this mixing is rotated away. The corresponding rotation matrix depends exclusively on CP-phases and it takes the form,

$$R_{\rm cp} = \begin{pmatrix} c_\theta & 0 & 0 & s_\theta & 0 \\ 0 & c_{\delta-3\theta} & 0 & 0 & s_{\delta-3\theta} \\ 0 & 0 & 1 & 0 & 0 \\ -s_\theta & 0 & 0 & c_\theta & 0 \\ 0 & -s_{\delta-3\theta} & 0 & 0 & c_{\delta-3\theta} \end{pmatrix} . \tag{23}$$

As the result of this rotation, the mass matrix takes the following block diagonal form,

$$M_s^2 = R_{\rm cp} M^2 R_{\rm cp}^T = \begin{pmatrix} M^2_{\rm scal} & 0 \\ 0 & M^2_{\rm pscal} \end{pmatrix} , \tag{24}$$

where

$$M^2_{\rm scal} = \frac{v_S^2}{2} \begin{pmatrix} \lambda_S - 3\lambda_{\rm cp}\omega & 3\lambda_{\rm cp} - 2\lambda_5\omega & 2\epsilon\lambda_{HS} \\ 3\lambda_{\rm cp} - 2\lambda_5\omega & \dfrac{(\lambda_{\rm cp} + \lambda_X\omega^3)}{\omega} & -2\epsilon\lambda_{HX}\omega \\ 2\epsilon\lambda_{HS} & -2\epsilon\lambda_{HX}\omega & \epsilon^2\lambda_H \end{pmatrix} \tag{25}$$

corresponds to the scalar mass matrix in the limit $\delta, \theta \to 0$, and the same happens for the pseudoscalar mass matrix,

$$M^2_{\rm pscal} = \frac{v_S^2}{2}\,\lambda_{\rm cp} \begin{pmatrix} 9\omega & 3 \\ 3 & \omega^{-1} \end{pmatrix} , \tag{26}$$

for vanishing CP-phases.

The model has 5 mass eigenstates labeled as $\zeta_i, i = 1 \ldots 5$. The first 2 correspond to those from $M^2_{\rm pscal}$, the rest comes $M^2_{\rm scal}$ where $\zeta_5$ is reserved to the SM-like higgs with a mass of $m_{\zeta_5} = m_h = 125$ GeV.

The pseudoscalar mass matrix has two eigenstates which are obtained by $R_{\rm pscal} M_{\rm pscal} R^T_{\rm pscal} = diag(m_{\zeta_1}, m_{\zeta_2})$ where

$$R_{\rm pscal} = \frac{1}{\sqrt{1+9\omega^2}} \begin{pmatrix} 1 & -3\omega \\ 3\omega & 1 \end{pmatrix} . \tag{27}$$

The $\zeta_1$ state corresponds to the goldstone boson of the $U(1)_l$ breaking and it is commonly known as *massless* majoron. The second eigenstate has a mass of

$$m^2_{\zeta_2} = M_J^2 = \frac{v_S^2}{2\omega}\lambda_{\rm cp}(1+9\omega^2) , \tag{28}$$

and it can be thought as a *massive* majoron. This state will be considered as the DM candidate of the model and we label it as $\zeta_2 = J_{\rm DM}$. For the purpose of this work, we will keep its mass around the keV range. Therefore it turns out to be $\lambda_{\rm cp} \simeq \frac{M_J^2}{v_S^2} < 10^{-22}$ for $\omega \simeq \mathcal{O}(1)$ and $v_S > 50$ TeV.

On the other hand, the scalar mass matrix provides 3 massive states which can be found by means of a perturbative diagonalization by using $\frac{M_J^2}{v_S^2}$ and $\epsilon$ as perturbative parameters. In that expansion, the SM-like higgs has a mass of

$$m_h^2 \simeq \frac{v_h^2}{2}\left\{\frac{\lambda_H}{2} + 2\left(\frac{\lambda_{HX}^2\lambda_S + \lambda_{HS}^2\lambda_X - 4\lambda_5\lambda_{HS}\lambda_{HX}}{4\lambda_5^2 - \lambda_S\lambda_X}\right)\right\}, \tag{29}$$

which is valid within this limit. The constraint due to the higgs mass provides restrictions on the values of the couplings of the second term (Eq. 29).

A simplified version for the constraint arises when taking $\lambda_5 = 0$ i.e. $\sigma_S$ and $\sigma_X$ as quasi-decoupled states. In this case, the higgs mass is

$$m_h^2 \simeq \frac{v_h^2}{2}\left\{\frac{\lambda_H}{2} - 2\left(\frac{\lambda_{HX}^2}{\lambda_X} + \frac{\lambda_{HS}^2}{\lambda_S}\right)\right\}, \tag{30}$$

and it gets a contribution from the couplings $\lambda_{HX}$, $\lambda_{HS}$, $\lambda_X$, and $\lambda_S$. Regardless of the size of the couplings, the mixing between $\sigma_h$ and $\sigma_S$–$\sigma_X$ is suppressed by terms $\mathcal{O}(\epsilon)$, this produces that $\zeta_5 = \sigma_h + \mathcal{O}(\epsilon)\cdot(\sigma_{S,X})$ and thus the $\zeta_5$ is mostly SM-like higgs. Nevertheless, throughout the paper we will stick to the limit $\lambda_{HX}$, $\lambda_{HS} \ll 1$, which guarrantees a higgs-like $\zeta_5$ as well and a small mixing of $\sigma_h$ with $\sigma_S$–$\sigma_X$.

In the same perturbative scheme, the remaining 2 massive states ($\zeta_{3,4}$) have masses:

$$M_{\zeta_3}^2 \simeq \frac{v_S^2}{2}\left(\frac{-A + A\psi + 2\lambda_X\omega\psi}{2\psi}\right), \tag{31}$$

$$M_{\zeta_4}^2 \simeq \frac{v_S^2}{2}\left(\frac{A + A\psi + 2\lambda_X\omega\psi}{2\psi}\right), \tag{32}$$

where $A$ and $\psi$ come from:

$$\lambda_S = A + \lambda_X\omega^2, \tag{33}$$

$$\lambda_5 = -A\left(\frac{\sqrt{1-\psi^2}}{4\,\omega\,\psi}\right). \tag{34}$$

The $A$ parameter can be seen as an alignment between $\lambda_S$ and $\lambda_X$ and therefore it has a range value of a typical adimensional coupling. The $\psi$ term is $\cos(\phi/2)$ where $\phi$ is the mixing angle of the sector $\sigma_S$ and $\sigma_X$, and since it is a trigonometric function, $\lambda_5$ can take positive and negative values. Without imposing any fine tunning of $A$ and $\psi$, the mass values for $\zeta_{3,4}$ are expected to be $\mathcal{O}(v_S)$.

The mass spectrum of the scalar sector has 3 well defined mass scales. First, we have the light states ($< \mathcal{O}(\text{keV})$) corresponding to the massless and massive majorons. The second scale is determined by the mass of SM-like higgs. And the last one corresponds to the states $M_{\zeta_3}$ and $M_{\zeta_4}$, given by $v_S$ ($> 50$ TeV).

## 3. Majoron dark matter

As it was shown in the previous section, our dark matter candidate corresponds to the *massive* majoron state ($J_{\text{DM}}$). In our model, the $J_{\text{DM}}$ is a decaying DM candi-

date [30, 43, 14] where its decay channels are mainly to neutrinos and *massless* majorons. In this section, we focus on these modes and also on the majoron dark matter production in the Early Universe.

### *3.1. Dark matter decay*

In the case of decaying DM, the main phenomenological constraint comes from the DM lifetime. We assume in our case that the majoron DM has a lifetime $\tau_{\rm DM} > 10^{27}$ s ($\Gamma_{\rm DM} < 10^{-52}$ GeV) [44]. Besides, in this model, we have two classes of decay modes: fermionic and scalar. The first one comes from Eq. 7 and corresponds to $J_{\rm DM} \to \nu\nu$, which is also the typical majoron signature [30, 43, 14, 45]. The second class corresponds to scalar modes coming from the potential (Eq. 16). In this case, they are 2-body decays ($J_{\rm DM} \to \zeta_i\zeta_j$) and 3-body decays ($J_{\rm DM} \to \zeta_i\zeta_j\zeta_k$). Since we assume a keV majoron, these modes are reduced to $J_{\rm DM} \to 2\zeta_1$ and $J_{\rm DM} \to 3\zeta_1$.

*3.1.1. Decay into neutrinos:* The decay rate to neutrinos from $J_{\rm DM}$ in this model is

$$\Gamma_\nu \simeq \frac{M_J}{32\pi}\left(||O_L||^2 + ||O_R||^2\right) , \tag{35}$$

where $m_\nu \ll M_J$ is taken. The terms $O_L$ and $O_R$ are the couplings to neutrinos which come from the $J_{\rm DM}$ projection on the scalar states $H, S, X$ and $\nu$ projection on the fermionic states $\nu_L, N_{1,2}$. The decay rate can be written in our model as

$$\Gamma_\nu = \frac{M_J}{32\pi} f\left(m_\nu, m_D, M, v_S\right) , \tag{36}$$

where the function $f$ is described in Appendix B.1 and it contains the dependence on the parameters of the couplings between neutrinos and the majoron DM.

The decay rate can be expanded in powers of $\frac{\mu}{M} = \alpha \sim 10^{-7}$, then, the expansion up to order $\alpha$ is:

$$\Gamma_\nu = \Gamma_{0\nu}(\omega)\left\{(2-3\omega^2)\left(2-3\omega^2(1+2\alpha)\right) + \mathcal{O}(\alpha^2)\right\} , \tag{37}$$

where the overall factor is:

$$\Gamma_{0\nu}(\omega) = \frac{M_J {m_\nu}^2}{256\pi v_S^2}\frac{1}{\omega^2(1+9\omega^2)} . \tag{38}$$

The decay rate vanishes for $\omega_0 = \sqrt{2/3}$ up to order $\alpha$ and the error carried by this choice produces a decay rate of $\Gamma_\nu = \Gamma_{0\nu}(\omega_0)\, 4\alpha^2$. This indicates that $v_X$ and $v_S$ should have similar values satisfying the previous ratio since further powers of $\alpha$ will act as perturbations around that value for $\omega_0$.

The overall factor can be evaluated at $\omega_0$ giving rise to:

$$\Gamma_{0\nu}(\omega_0) \simeq 10^{-40}\,\text{GeV}\left(\frac{m_\nu}{0.1\,\text{eV}}\right)^2\left(\frac{M_J}{1\,\text{keV}}\right)\left(\frac{v_S}{100\,\text{TeV}}\right)^{-2} , \tag{39}$$

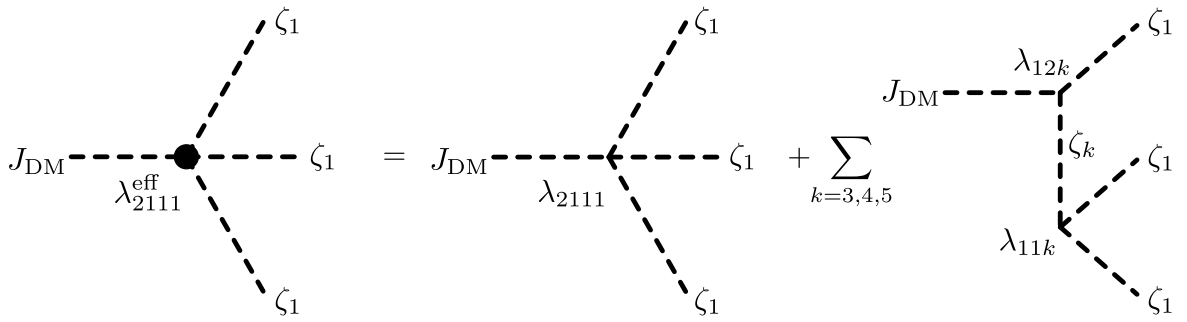


Figure 1: Diagrams involve in the calculation of $\lambda_{2111}$ for the process $J_{\rm DM} \to 3\zeta_1$

this indicates that we still require a factor $10^{-12}$ in order to satisfy the DM stability constraint. However, the $\Gamma_\nu$ at $\omega_0$ gets a $10^{-14}$ suppression due to the $\alpha^2$ factor. Hence it ensures that $\Gamma_\nu < \Gamma_{\rm DM}$. Nonetheless, the solution at all orders in $\alpha$ for $\Gamma_\nu = 0$ is exact and it is given by:

$$\omega = \frac{\sqrt{4 - 4\alpha^2 + \alpha^3 - \alpha^4}}{\sqrt{3(2 + 2\alpha + \alpha^4)}} \tag{40}$$

It is quite remarkable that the $\mu/M$ ratio is at the same time relevant for the neutrino mass value in the inverse seesaw mechanism and for the DM lifetime.

*3.1.2. Decay into scalars:* The scalar modes can occur only for $J_{\rm DM} \to 2\zeta_1$ and $J_{\rm DM} \to 3\zeta_1$ due to $M_J$ is $\mathcal{O}$(keV) and the heavy scalars have masses larger than 100 GeV. The couplings needed to calculate the decay rate come from the scalar potential after writing it in terms of the mass eigenstates and taking the corresponding derivatives:

$$\lambda_{ijk} = \frac{\partial^3 V_{\rm scalar}}{\partial\zeta_i \partial\zeta_j \partial\zeta_k} \quad \text{and} \quad \lambda_{ijkl} = \frac{\partial^4 V_{\rm scalar}}{\partial\zeta_i \partial\zeta_j \partial\zeta_k \partial\zeta_l}\,. \tag{41}$$

Afterwards, the decay rate for the 3-body process can be calculated as

$$\Gamma_{3\zeta} = \frac{1}{(64\pi)^3} M_J \left|\left|\lambda^{\rm eff}_{2111}\right|\right|^2 \tag{42}$$

where $\lambda^{\rm eff}_{2111}$ includes the diagrams depicted in Fig. 1. Notice that the contributions for this coupling come directly from the scalar potential and from the combined contributions from the heavy scalars. Given a $J_{\rm DM}$ with a mass in the keV range, we can safely integrate out the effect of the heavy mediators giving rise to:

$$\lambda^{\rm eff}_{2111} = \lambda_{2111} - \frac{\lambda_{213}\lambda_{113}}{m_3^2} - \frac{\lambda_{214}\lambda_{114}}{m_4^2} - \frac{\lambda_{215}\lambda_{115}}{m_5^2}\,, \tag{43}$$

where the relevant expressions for $\lambda_{2ij}$ and $\lambda_{2111}$ are shown in Appendix B.2.

Our aim is to obtain $\lambda^{\rm eff}_{2111} \simeq 0$ in order to stabilize the DM. The first 3 terms come from Eq. 11 and they are mainly unsuppressed quartic couplings. On the other hand, we found that last term in Eq. 43 contains an overall factor of $(M_J/v_S)^4$ which comes

from Eq. 12. This last term, eventually, will provide the main contribution to the decay rate whether all the other terms are vanished, so that we can estimate a typical value of the decay rate when only this term is present. In such conditions, the decay is given by:

$$\begin{aligned}\Gamma_{3\zeta} &= \frac{1}{(64\pi)^3}\, M_J \left|\left| \frac{\lambda_{215}\lambda_{115}}{m_5^2} \right|\right|^2 \\ &= \frac{1}{(64\pi)^3}\, M_J \left(\frac{M_J}{v_S}\right)^8 \cdot \left(\frac{\psi^2\omega^3}{(1+9\omega^2)^3}\, \mathcal{F}\left(A, \psi, \omega, \lambda_h, \lambda_{HS}, \lambda_{HX}\right)\right)^2 ,\end{aligned} \tag{44}$$

where the function $\mathcal{F}\left(A, \psi, \omega, \lambda_h, \lambda_{HS}, \lambda_{HX}\right)$ goes to zero when both couplings $\lambda_{HS}$ and $\lambda_{HX}$ go to zero. For a wide range of the values of the couplings, we obtain that $\mathcal{F} \sim \mathcal{O}(1)$. This implies that the decay rate is suppressed mainly by $(M_J/v_S)^8$. Hence, an orders of magnitude evaluation of the decay rate is given by:

$$\Gamma_{3\zeta} \sim 10^{-12} \left(\frac{M_J}{1\,\text{keV}}\right)\left(\frac{M_J}{v_S}\right)^8 \text{GeV} \;\sim\; 10^{-100}\,\text{GeV}\,. \tag{45}$$

The last estimation indicates that $\Gamma_{3\zeta}$, when only the contribution of the higgs is considered, is larger than our benchmark for $\Gamma_{\text{DM}}$ by 48 orders of magnitude. This implies that the decay mediated does not spoil the DM lifetime whatsoever, and it can be safety neglected under our assumptions. Now our concern is to vanish the remaining terms in Eq. 43:

$$\lambda_{2111} \;-\; \lambda_{213}\lambda_{113}/m_3^2 \;-\; \lambda_{214}\lambda_{114}/m_4^2 \;\simeq\; 0\,. \tag{46}$$

The full expressions involved in this equation in the limit $\lambda_{HX},\, \lambda_{HS} \ll 1$ are given in Appendix B.2. The first term comes directly from the scalar potential and it is not necessarily suppressed. However it does contain terms proportional to $(M_J/v_S)^2$ that can be neglected. The last 2 terms are always present and require that $0 < \psi < 1$ to be well defined (see Eqs. B.9 and B.12). This condition forces to have a non-zero $\lambda_5$ via the value of $A$. At this point and due to the complexity of the expressions involved at Eq. 46, we will explore the parameter space with a numerical scan which we are going to discuss in the next section.

### *3.2. Dark matter production*

In this section, we aim to describe a tentative framework for the DM production in the Early Universe. Our DM candidate $J_{\text{DM}}$ shares similar properties with a Feebly Interacting Massive Particle (FIMP) [46] by means of suppressed coupling with the SM-like higgs and active neutrinos. However, the couplings of $J_{\text{DM}}$ to the heavy scalars $\zeta_3$ and $\zeta_4$ may not be necessarily suppressed, and in turn, the couplings of these particles with the SM-like higgs might take a wide range of values. This makes the heavy scalars to be able to interact with the rest of the thermal bath, and subsequently decay to $J_{\text{DM}}$. Indeed, the same logic could be applied to the process involving heavy neutrinos. Under these conditions, and since we assume a keV DM candidate, the production mechanism

cannot be addressed with the typical freeze-out for $J_{\rm DM}$, which is used in WIMP-DM models to reproduce the relic abundance [47].

On top of having $J_{\rm DM}$ as a FIMP, the Lightest Observable Sector Particle (LOSP) could be either the lighest of the heavy neutrinos or the lightest between $\zeta_{3,4}$ because all of them have $U(1)_l$ charges. Due to the interplay among all particles of the model, the relic abundance calculation has many edges which at first sight are unclear, however, we will sketch some relevant processes involved in the production.

Some of the prototype processes for the DM production can be summarized either by a quartic interaction like $\lambda\,\zeta_3\zeta_4 J_{\rm DM}^2$ and $\dfrac{\lambda'}{v_S}\overline{\mathcal{N}}\mathcal{N}' J_{\rm DM}^2$, or a triple interaction like $y\overline{\mathcal{N}}\mathcal{N}' J_{\rm DM}$ and $\lambda'' v_S\,\zeta_3\zeta_1 J_{\rm DM}$.

Focusing now only on the couplings of the scalar sector, we realize that the ones between $J_{\rm DM}$–$\zeta_{3,4}$, and $\zeta_{3,4}$–$\zeta_5$ are not necessarily suppressed, and they are controlled mainly by $\lambda_{X,S}$ and $\lambda_{HX,HS}$ respectively. Oppositely, the coupling in $J_{\rm DM}$–$\zeta_5$ is suppressed by the ratio $(M_J/v_S)^2$.

The lagrangian $\mathcal{L}_{\rm int} = y_L\bar{L}HN_1$, where the yukawa value is proportional to $m_D$, gives rise to the interactions $\nu\zeta_5\mathcal{N}^{(\prime)}$. Besides, the lagrangian $\mathcal{L}_{\rm int} = y_S S N_1 N_2$, where the coupling is proportional to $M$, gives rise to interactions $J_{\rm DM}\mathcal{N}^{(\prime)}\mathcal{N}^{(\prime)}$. In both cases, the couplings are controlled by the inverse seesaw and, in our setup, they are $y_L \simeq 0.1$ and $y_S \simeq 1$. All of this produces an interplay between neutrinos, higgs, and DM, similar to the scalar sector and the interplay among heavy scalars and majorons.

In the Early Universe, the evolution of the DM yield depends directly on the interaction of $\zeta_{3,4}$ and/or $\mathcal{N}^{(\prime)}$ with the SM. In this way, the yields of LOSPs act as portals between SM and DM. The combined processes are present meanwhile $T \gtrsim m_{\rm LOSP}$. This means that LOSPs are likely in thermal equilibrium. After that, they will decouple from the thermal bath in a similar way to the freeze-out, transferring subsequently their yields to $J_{\rm DM}$ and $\zeta_1$ via LOSP decays. However, not all of the final DM yield comes necessarily from these decays. If the DM-LOSP couplings are large enough, DM could reach thermal equilibrium assisted by LOSP's interactions and thus a fraction of the DM yield comes from the DM freeze-out. Otherwise, i.e. for small couplings, the outcoming fraction of the DM could be explained via freeze-in. A more complete calculation of the DM abundance will be given in a future work.

## 4. Discussion

Up to this moment, we have described the expression for the $J_{\rm DM}$ decay into neutrinos and three $\zeta_1$. However, in this section, we aim to perform numerical analysis based on the stability of the DM candidate since this is the observable that constraints most the couplings. Since we know the DM lifetime is extremely large and our model does not include a ad-hoc stabilizing symmetry, it is expected that the correlations among parameters must be strong. In any case, we could assume that the correlations are the consequence of an unknown unified symmetry. Moreover, in this part, we will not include

| Parameter | Value |
|---|---|
| $M$ | 100 TeV |
| $\mu$ | 10 MeV |
| $m_D$ | 10 GeV |
| $v_S$ | $10^8$ – $10^{12}$ GeV |
| $\omega$ | 0.4 – 1.6 |

Table 2: Benchmarks and scan range for parameters in the $J_{\rm DM} \to \nu\nu$ decay.

constraints coming from the DM relic abundance.

In the first place, the channel to neutrinos will be analyzed. As we can see from Appendix B.1, the formuli regarding the couplings $O_L$ and $O_R$ shown at the Eq. 35 just depend on the parameters $m_D$, $M$, $\omega$, $v_S$, and $m_\nu$. Although in this case, a dependence on the mass of the neutrino appears in order to make the parameter space compatible with $m_\nu \sim 0.1$ eV (See Tab. 2). It is evident to realize that vanishing couplings imply a vanishing amplitude $\Gamma\left(J_{\rm DM} \to 2\nu\right)$. Thus, given a set of $M$, $m_D$ and $v_S$, one can search for an $\omega$ that makes $J_{\rm DM}$ decay to neutrinos in cosmological times. In Fig. 2, we present the result of a scan on the $J_{\rm DM}$ decay width in the plane: $v_S$ versus $\omega$. We showed in Eq. 40 that $\omega \simeq \sqrt{2/3}$ makes the couplings $O_L$ and $O_R$ vanish. In this plot, we present the decay width variability for a range of $\omega$ values. We highlight, with the dashed line, the frontier of the DM lifetime. For smaller values of $v_S$, DM lifetime requires that omega must be very close to $\sqrt{2/3}$, indicating a rather strong vev alignment among $S$ and $X$. In opposition, larger values of $v_S$ weakens this alignment, since there is an overall factor $v_S^{-2}$ in the decay width (Eq. 37).

In the analysis of the scalar decay, as it was described in the previous section, the approach is to vanish the non-Higgs part of the coupling $\lambda^{\rm eff}_{2111}$ (i.e. Eq. 46). The Higgs part is neglected because it is extremely suppressed. Besides, the scalar sector parameter space is mostly independent of the fermion sector, although it is connected by $\omega$ and $v_S$. Thus, we look for an interplay among the parameters $A$, $\psi$, $\lambda_X$, and $\omega$ that satisfies Eq. 46.

In Fig. 3, we show the combinations of $\psi$ and $\omega$ that vanish the decay width for 2 values of $A = (0.2, 0.5)$ and 5 for $\lambda_X$ in different shades of blue. This selection was made in order to show a general trend in the dependence between $\psi$ and $\omega$. The blue curves range from the largest possible $\lambda_X$ (lightest blue line) given by the perturbation limit, to a smaller value ($\lambda_X = 0.1$, darkest blue). The left-most value of each curve indicates a solution when $\psi$ starts to become complex or stops to represent a cosine of an angle. The light green zone corresponds to the range of $\omega$ compatible with the decay to neutrinos for $v_S \sim 10^{11}$ GeV. The vertical dashed line is simply $\omega = \sqrt{2/3}$. The scanned range of $\omega$ was up to 3 in order to explore a ratio $v_X$ more or less in the same order of magnitude of $v_S$. Besides, we include the constraint that the heaviest scalars are above the TeV

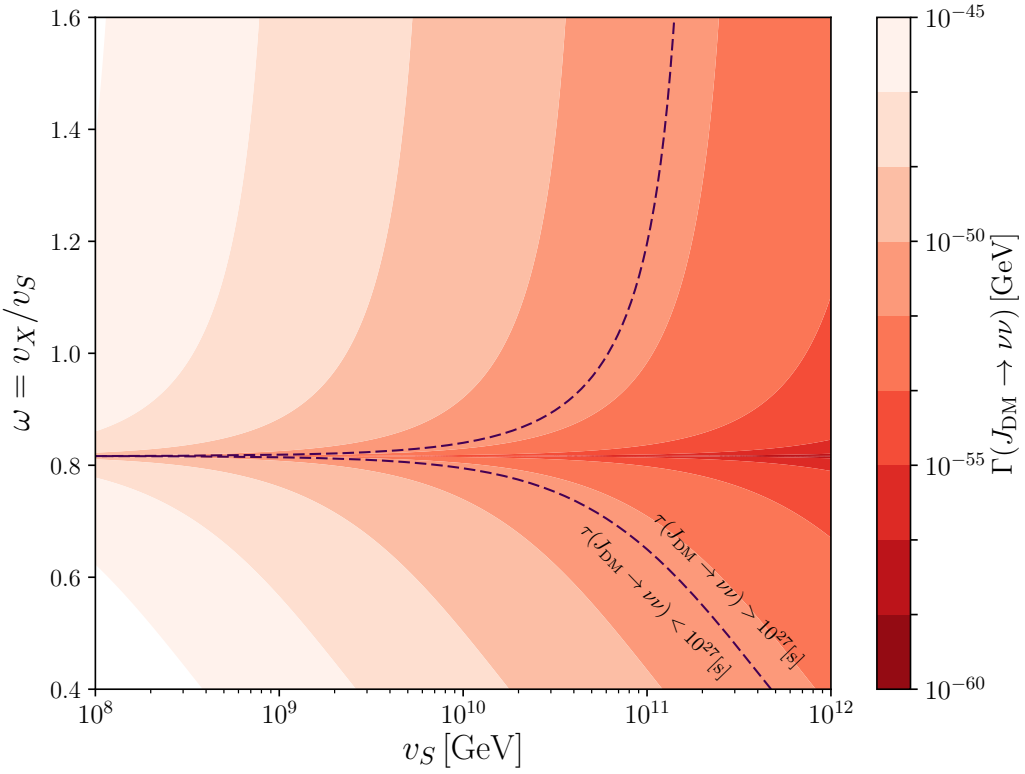


Figure 2: Plot $v_S$ versus $\omega$. The color palette indicates the value of the $J_{\rm DM}$ decay width to neutrinos. The dashed line shows the benchmark value for the DM lifetime $\tau_{DM} = 10^{27}$ s. The value $\omega = \sqrt{2/3}$ makes the decay width vanish regardless of $v_S$ value. For $v_S \gg 10^{11}$ GeV, $\omega$ starts to be irrelevant to satisfy the DM lifetime constraint.

scale.

By comparing both plots in Fig. 3, we observe that the perturbative limit for $\lambda_X$ sets a minimum $\psi(\omega)$-curve. This minimum curve grows with larger values of $A$. In opposition, the maximum $\psi(\omega)$-curves are related with the smallness of $\lambda_X$, however $\lambda_X \simeq 0$ puts problems with the vacuum stability. Similar information is shown in Fig. 4, where we present the zero decay width solution for $A$ versus $\omega$. Here we observe that the pertubative limit of $\lambda_X$ produces a maximum $A(\omega)$-curve for each choice of $\psi$.

For both Figs. 3 and 4, we show that there is a smooth transition for different values of $\lambda_X$ and the combinations of $\psi$, $A$, and $\omega$ that make the decay width zero. This implies that the solutions belong to a smooth volume in the parameter space, and therefore, one can always find one parameter when the other 3 have been given. Besides, we find that extreme values of $A\,(\sim 0)$, and $\psi\,(\gtrsim 1.0\,, \lesssim 0.0)$, are not favored by the DM stability condition and these values could lead to tachyonic states of $\zeta_3$ or $\zeta_4$. Moreover, when we focus on the green region, we find that the most of the curves pass through it. This is showing that there is a natural compatibility among the solutions for the neutrino and

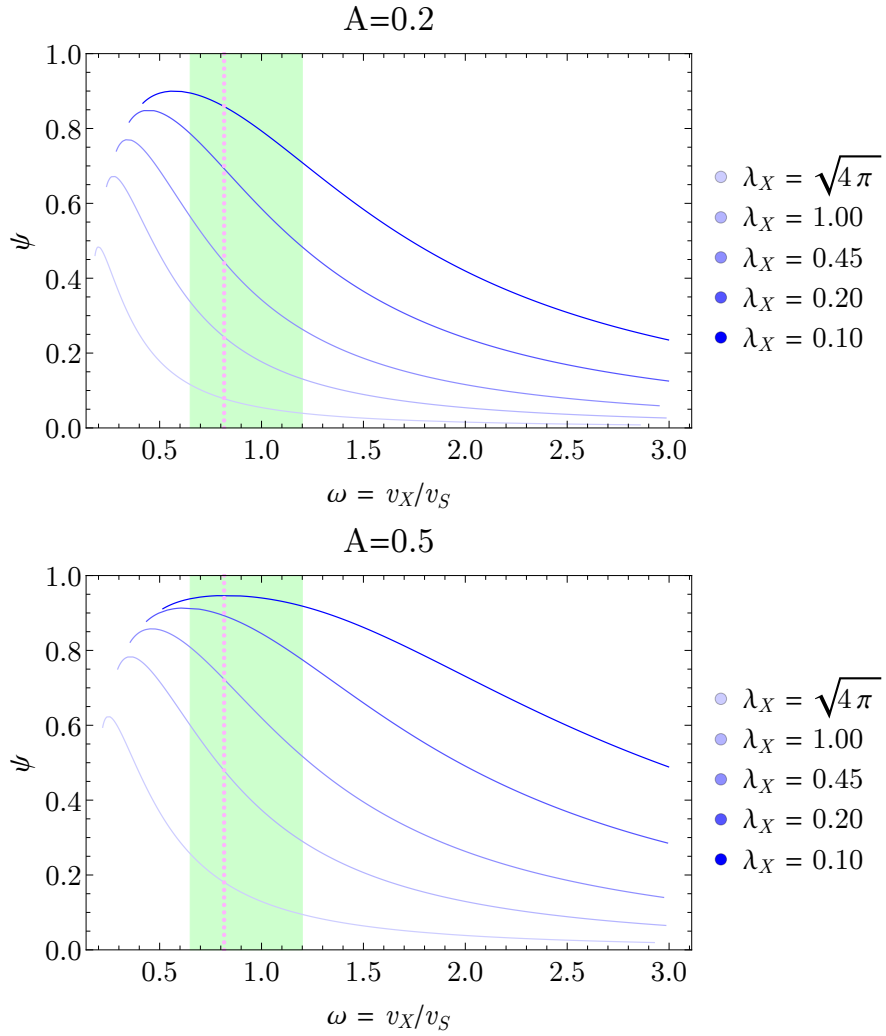


Figure 3: Plot $\psi$ versus $\omega$ for $A = 0.2$ (top) and $A = 0.5$ (bottom). The bluish lines correspond for the combination of $\psi$ and $\omega$ for a fixed value of $\lambda_X$ that makes the decay $J_{\rm DM} \to 3\zeta_1$ zero. The vertical magenta dashed line correspond to $\omega = \sqrt{2/3}$. The green area is the $\omega$ range that passes the DM lifetime constraint for the neutrino channel for $v_S \simeq 10^{11}$ GeV.

scalar decay modes independently.

An interesting case regards the higgs physics, in our model the mixing among the CP-even scalars gives a SM-like higgs that is weakly mixed with the rest of the scalars by a factor $v_h/v_S$. However, this mixing does not forbid a contribution to the invisible higgs decay, namely $H \to J_{\rm DM}J_{\rm DM}$, $J_{\rm DM}\zeta_1$, $\zeta_1\zeta_1$. These processes come directly from the scalar potential via couplings $\lambda_{HS}$, $\lambda_{HX}$, and $\lambda_{\rm cp}$, which are translated into $\lambda_{215}$, $\lambda_{115}$, and $\lambda_{225}$ (See Eqs. B.18, B.19, and B.20, respectively). We observe that all these couplings are suppressed by $(M_J/v_S)^2$, therefore the decay width is suppressed by $(M_J/v_S)^4$. After evaluation, we obtain that the higgs decay width is $\mathcal{O}\,(10^{-44})$ GeV and thus these processes cannot be constrained using the measurement of the invisible higgs

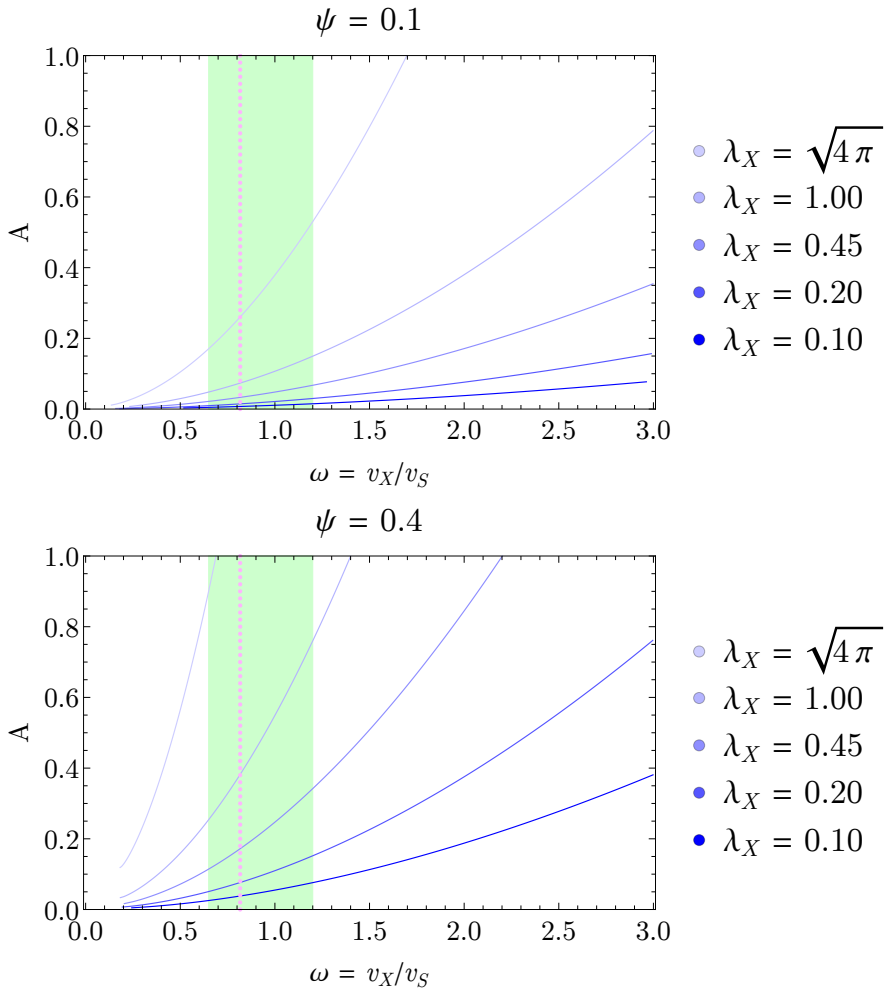


Figure 4: Plot $A$ versus $\omega$ for $\psi = 0.1$ (top) and $\psi = 0.4$ (bottom). The bluish lines correspond for the combination of $A$ and $\omega$ for a fixed value of $\lambda_X$ that makes the decay $J_{\rm DM} \to 3\zeta_1$ zero. The vertical magenta dashed line correspond to $\omega = \sqrt{2/3}$. The green area is the $\omega$ range that passes the DM lifetime constraint for the neutrino channel for $v_S \simeq 10^{11}$ GeV.

decay [48, 49].

The role of CP-phases in the decay width either in the scalar or neutrino modes is not an issue. In the scalar sector, most of the effect is washed out by the tadpole equations that fix the relation among the 3 phases: $\theta$, $\tau$, and $\delta$. In the case of neutrinos, in addition to our CP-phases, we could include extra phases in the yuwakas: $y_L$, $y_S$, and $y_X$. However, we decided to keep the inverse seesaw mass terms real, and hence, the possible impact of CP-phases in the phenomenology is absorbed. If we wanted to add effect of CP-phase, we should either relax the condition of real mass terms or add more families of neutrinos.

This addition of CP-phases effects in the DM decay adds an improvement on this setup. A different improvement is to promote from a global $U(1)_l$ symmetry to a gauge

one. This would relax the correlations in the scalar sector, because the $\zeta_1$ would be eaten by the corresponding gauge boson after the SSB. The latter feature is going to be worked out in a future work.

## 5. Conclusions

In this work, we propose an extension of SM where neutrinos are Majorana particles and they become massive through an inverse seesaw mechanism which arises from the spontaneous symmetry breaking of the lepton number. Our model allows us to have a massive Majoron as a DM candidate. This latter particle has the following characteristics: *i)* Its mass comes from the mixing in the pseudoscalar sector. The mixing arises due to the lepton number charges needed by the neutrino and scalar sectors to make the lagrangian invariant under lepton number. The mass range could go from the keV's up to TeV's, although we have explored just the keV region. *ii)* It is metastable and its main decay channels are to neutrinos and massless Majorons. These channels are similar to models with Majorons as *pseudo-goldstone bosons*. For simplicity, we test the model assuming one family of active neutrinos, although the extension to 3 families can be easily implemented.

The introduced scalars, that give rise to the inverse seesaw mechanism, also allow the spontaneous breaking of CP invariance. Nevertheless the effect is not present in our model's phenomenology because we included just one family of active neutrinos.

The DM candidate stability is very fragile in this model because we did not include any *ad-hoc* stabilizing symmetry. However, we found that there is always a region in the parameter space where the massive Majoron has a lifetime longer than $10^{27}$ s and, therefore, it can be considered as a good DM candidate.

Moreover, we found that the ratio among vevs, $\omega$, has a very important role in the decay channel to neutrinos. The value $\omega = \sqrt{2/3}$ can vanish the decay mode to neutrinos presenting a tantalizing vev alignment for model building. The scalar decay modes are the most crucial because the drastical effect on the total DM lifetime and from the point of view of scan of the parameter space. Nevertheless, we found that the decay width vanished in a region of the parameter space of the scalar sector. We also discussed how to rid off the scalar decay modes by promoting the global lepton symmetry to a local one. We discuss possible ways on how to estimate the DM relic abundance in terms of a freeze-in scenario.

In general words, the model presents an interesting relation between the neutrino mass mechanism and origin of the massive Majoron as a DM candidate.

## Appendix A. Lepton charge assignments

In this section, we examine the most general way in which the lepton charges are fixed for the fields $N_1$, $N_2$, $S$ and $X$. As we advanced, the Yukawa couplings at Eq. 7 will fix the value for the lepton numbers of the field $N_1$. However, this does not fix the

charges for the new scalars $S$ and $X$, nor for $N_2$. The final assignation can be obtained after considering the following general scalar potential:

$$V_{\rm I} = \lambda_{\rm cp} e^{i\delta} X^m S^{\dagger n} + \text{h.c.}\,, \tag{A.1}$$

After demanding that $V_I$ is renormalizable, we can choose the values of $m$ and $n$ that subsequently will fix the values of lepton number for $S$ and $X$. Thus, one has a collection of models formed by taking $m+n = 2, 3, 4$. Notice that we still have to choose one value for $m$ and $n$. By now, we choose $m + n = 4$ and, by following the assignation made at the Table 1, we establish conditions in order to make A.1 invariant under lepton number.

$$\begin{aligned} &m \,+\, n \,=\, 4 \quad \text{and} \quad m\,(2x) \,-\, n\,(1 \,-\, x) \,=\, 0 \quad \Rightarrow \\ &x \,=\, \frac{n}{n+2m} \,=\, \frac{n}{8-n} \end{aligned} \tag{A.2}$$

Recall that $n, m$ are integers running from $1 \ldots 3$ (0 and 4 will break lepton number explicitly). Therefore, for $n = 3$ and $m = 1$, one has $x = 3/5$, as it was stated in the section 2.2. At the Table A1, we present the lepton number charges for different values of $n$ for $m + n = 4$. In order to show a case with a different choice of $m + n$, at the Table A2 we present the lepton numbers of the fields after considering $m + n = 3$ at Eq. A.1.

## Appendix B. Couplings

In this section we describe briefly the relevant couplings used in this work, with an special emphasis in the interactions participating in the decays of the Majoron.

| | $L$ | $N_1$ | $N_2$ | $S$ | $X$ |
|---|---|---|---|---|---|
| $n = 1$ | 1 | $-1$ | 1/7 | 6/7 | 2/7 |
| $n = 2$ | 1 | $-1$ | 1/3 | 2/3 | 2/3 |
| $n = 3$ | 1 | $-1$ | 3/5 | 2/5 | 6/5 |

Table A1: Charge assignment of different models for $m + n = 4$.

| | $L$ | $N_1$ | $N_2$ | $S$ | $X$ |
|---|---|---|---|---|---|
| $n = 1$ | 1 | $-1$ | 1/5 | 4/5 | 2/5 |
| $n = 2$ | 1 | $-1$ | 1/2 | 1/2 | 1 |

Table A2: Charge assignment of different models for $m + n = 3$.

*Appendix B.1. Fermion Couplings*

The couplings shown below are related to the process $J_{DM} \longrightarrow \nu\nu$ that appears in the models involving majoron DM. Recall that in these couplings we got rid of the explicit dependence of the Yukawas and it was preferred to work with the mass parameters involved in neutrino mass generation via inverse seesaw, namely $\mu$, $m_D$ and $M$ (c.f. Eq. 35)

$$O_L = \frac{\mathcal{D}_1^{(L)}}{\mathcal{D}_2^{(L)}} \tag{B.1}$$

$$\begin{aligned}\mathcal{D}_1^{(L)} = & \, im_\nu \left(4m_D^6 + 4Mm_D^4 m_\nu + M^3 m_\nu^3\right) \\ & \left[\left(-4m_D^8 + 4M^2 m_D^4 m_\nu^2 - M^3 m_D^2 m_\nu^3 + M^4 m_\nu^4\right)\right. \\ & + \left. 3\left(2m_D^8 + 2Mm_D^6 m_\nu + M^4 m_\nu^4\right)\omega^2\right]\end{aligned} \tag{B.2}$$

$$\begin{aligned}\mathcal{D}_2^{(L)} = & \left(2m_D^2 + 3Mm_\nu\right)^2 \left(m_D^2 - Mm_\nu\right) \\ & \left(2m_D^4 - Mm_D^2 m_\nu + M^2 m_\nu^2\right)^2 v_s \omega \sqrt{2 + 18\omega^2}\end{aligned} \tag{B.3}$$

$$O_R = \left(O_L\right)^* . \tag{B.4}$$

By using the definitions from above, the function $f$ at Eq. 36 can be expressed as

$$f\left(m_\nu, m_D, M, v_S\right) = ||O_L||^2 + ||O_R||^2 \tag{B.5}$$

*Appendix B.2. Scalar Couplings*

Since the relevant couplings for the DM decay in the scalar sector are cuartic, they have no mass dimensions. This is respected by the effective coupling at Eq. 43, which makes the entire coupling independent of mass scales, and thus, it just depends on the adimensional parameters we set (namely $A$, $\omega$, $\psi$, $\lambda_h$, $\lambda_X$ and $M_J/v_S$).

First, it is shown the formula for the direct contribution to this coupling:

$$\lambda_{2111} = \frac{\mathcal{D}_1^{(1)}}{\mathcal{D}_2^{(1)}} \tag{B.6}$$

$$\begin{aligned}\mathcal{D}_1^{(1)} = & -3\left[3A\left(1 + 9\omega^2\right)\left\{-2\psi\omega + \sqrt{1 - \psi^2}\left(-1 + 9\omega^2\right)\right\}\right. \\ & + \left. 8\psi\omega\left\{\left(\frac{M_J^2}{v_s^2}\right) - 27\left(\frac{M_J^2}{v_s^2}\right)\omega^2 + 6\lambda_X\omega^2\left(1 + 9\omega^2\right)\right\}\right]\end{aligned} \tag{B.7}$$

$$\mathcal{D}_2^{(1)} = 4\psi(1 + 9\omega^2)^3 \tag{B.8}$$

Now, we show the formuli for the contributions coming from the integrated effect of the heavy scalars. On the one hand, we explicit the formuli for $\frac{\lambda_{213}\lambda_{113}}{m_3^2}$ and $\frac{\lambda_{214}\lambda_{114}}{m_4^2}$, which share some similarities.

$$\frac{\lambda_{213}\lambda_{113}}{m_3^2} = \frac{\mathcal{D}_1^{(3)}}{\mathcal{D}_2^{(3)}} \tag{B.9}$$

$$\begin{aligned}
\mathcal{D}_1^{(3)} &= 3\Big[A\left(-1+\psi\right)\left(-1+\psi-9\sqrt{1-\psi^2}\omega\right)\left(1+9\omega^2\right) \\
&- 2\psi\omega\left(12\left(\frac{M_J^2}{v_s^2}\right)\left(\sqrt{1-\psi^2}+5\left(-1+\psi\right)\omega\right)\right. \\
&+ \left.\lambda_X\omega\left(1-\psi+9\sqrt{1-\psi^2}\omega\right)\left(1+9\omega^2\right)\right)\Big] \\
&\Big[A\left(-1+\psi\right)\left(\sqrt{1-\psi^2}+\left(-1+\psi\right)\omega\right)\left(1+9\omega^2\right) \\
&+ 2\psi\omega\left(\lambda_X\omega\left(\sqrt{1-\psi^2}+\left(-1+\psi\right)\omega\right)\left(1+9\omega^2\right)\right. \\
&- \left.4\left(\frac{M_J^2}{v_s^2}\right)\left(1+3\sqrt{1-\psi^2}\omega-6\omega^2+\psi\left(-1+6\omega^2\right)\right)\right)\Big]
\end{aligned} \tag{B.10}$$

$$\begin{aligned}
\mathcal{D}_2^{(3)} &= 8\left(-1+\psi\right)\psi\left(1+9\omega^2\right)^3 \\
&\left[-A\left(1+\psi\right)\left(1+9\omega^2\right)+2\psi\left(-\lambda_X\omega^2\left(1+9\omega^2\right)\right.\right. \\
&+ \left.\left.\left(\frac{M_J^2}{v_s^2}\right)\left(-1+\psi-6\sqrt{1-\psi^2}\omega+3\omega^2+3\psi\omega^2\right)\right)\right],
\end{aligned} \tag{B.11}$$

$$\frac{\lambda_{214}\lambda_{114}}{m_4^2} = \frac{\mathcal{D}_1^{(4)}}{\mathcal{D}_2^{(4)}} \tag{B.12}$$

$$\begin{aligned}
\mathcal{D}_1^{(4)} &= 3\Big[A\left(1+\psi\right)\left(1+\psi-9\sqrt{1-\psi^2}\omega\right)\left(1+9\omega^2\right) \\
&- 2\psi\omega\left(12\left(\frac{M_J^2}{v_s^2}\right)\left(\sqrt{1-\psi^2}+5\left(1+\psi\right)\omega\right)\right. \\
&- \left.\lambda_X\omega\left(1+\psi-9\sqrt{1-\psi^2}\omega\right)\left(1+9\omega^2\right)\right)\Big] \\
&\Big[A\left(1+\psi\right)\left(\sqrt{1-\psi^2}+\omega+\psi\omega\right)\left(1+9\omega^2\right) \\
&+ 2\psi\omega\left(\lambda_X\omega\left(\sqrt{1-\psi^2}+\omega+\psi\omega\right)\left(1+9\omega^2\right)\right. \\
&- \left.4\left(\frac{M_J^2}{v_s^2}\right)\left(-1+3\sqrt{1-\psi^2}\omega+6\omega^2+\psi\left(-1+6\omega^2\right)\right)\right)\Big]
\end{aligned} \tag{B.13}$$

$$\begin{aligned}
\mathcal{D}_2^{(4)} &= 8\psi\left(1+\psi\right)\left(1+9\omega^2\right)^3 \\
&\left[A\left(-1+\psi\right)\left(1+9\omega^2\right)+2\psi\left(\lambda_X\omega^2\left(1+9\omega^2\right)\right.\right. \\
&+ \left.\left.\left(\frac{M_J^2}{v_s^2}\right)\left(1+\psi-6\sqrt{1-\psi^2}\omega-3\omega^2+3\psi\omega^2\right)\right)\right]
\end{aligned} \tag{B.14}$$

The contributions of the Higgs field to the majoron decay (the fraction $\frac{\lambda_{215}\lambda_{115}}{m_5^2}$) are written below. The expressions for $\lambda_{215}$, $\lambda_{225}$ and $\lambda_{115}$ are proportional to the ratio

$\left(\frac{M_J}{v_s}\right)^4$, thus, having a keV majoron implies a natural supression for the contributions to the decay.

$$\frac{\lambda_{215}\lambda_{115}}{m_5^2} = \frac{\mathcal{D}_1^{(5)}}{\mathcal{D}_2^{(5)}} \tag{B.15}$$

$$\begin{aligned}
\mathcal{D}_1^{(5)} &= -1152\left(\frac{M_J}{v_S}\right)^4 \psi^2\omega^3\left[2\psi\left(5\lambda_{HS}-\lambda_{HX}\right)\lambda_X\omega^3\right. \\
&- \left. A\left\{\sqrt{1-\psi^2}\lambda_{HS}+\lambda_{HX}\omega\left(2\psi-5\sqrt{1-\psi^2}\omega\right)\right\}\right] \\
&\left[-2\psi\lambda_X\omega\left(\lambda_{HS}-6\lambda_{HS}\omega^2+3\lambda_{HX}\omega^2\right)\right. \\
&- \left. A\left\{3\sqrt{1-\psi^2}\lambda_{HS}+\lambda_{HX}\left(6\psi\omega+\sqrt{1-\psi^2}\left(1-6\omega^2\right)\right)\right\}\right]
\end{aligned} \tag{B.16}$$

$$\begin{aligned}
\mathcal{D}_2^{(5)} &= \left(1+9\omega^2\right)^3 \\
&\left[-A^4\left(-1+\psi^2\right)^2\lambda_h\left(1+9\omega^2\right)+8A^3\psi\left(-1+\psi^2\right)\omega\right. \\
&\left.\left(2\sqrt{1-\psi^2}\lambda_{HS}\lambda_{HX}+\psi\left(2\lambda_{HX}^2-\lambda_h\lambda_X\right)\omega\right)\left(1+9\omega^2\right)\right. \\
&+ 16\psi^4\lambda_X^2\omega^6\left[8\left(\frac{M_J}{v_S}\right)^2\left(3\lambda_{HS}^2+6\lambda_{HS}\lambda_{HX}-\lambda_{HX}^2\right)\right. \\
&+ \left.\left.\lambda_X\left(1+9\omega^2\right)\left(4\lambda_{HS}^2+\left(4\lambda_{HX}^2-\lambda_h\lambda_X\right)\omega^2\right)\right] \\
&+ 32A\psi^3\lambda_X\omega^3\left[\lambda_X\omega\left(1+9\omega^2\right)\left\{2\sqrt{1-\psi^2}\lambda_{HS}\lambda_{HX}\omega\right.\right. \\
&+ \left.\psi\left(2\lambda_{HS}^2+\left(4\lambda_{HX}^2-\lambda_h\lambda_X\right)\omega^2\right)\right\} \\
&+ 4\left(\frac{M_J}{v_S}\right)^2\left\{3\sqrt{1-\psi^2}\lambda_{HS}^2+\lambda_{HX}^2\omega\left(-2\psi+3\sqrt{1-\psi^2}\omega\right)\right. \\
&+ \left.\left.\lambda_{HS}\lambda_{HX}\left(6\psi\omega+\sqrt{1-\psi^2}\left(-1+3\omega^2\right)\right)\right\}\right] \\
&+ 8A^2\psi^2\left\{\lambda_X\omega^2\left(1+9\omega^2\right)\left(2\left(-1+\psi^2\right)\lambda_{HS}^2\right.\right. \\
&+ \left.8\psi\sqrt{1-\psi^2}\lambda_{HS}\lambda_{HX}\omega+\left(2\left(-1+5\psi^2\right)\lambda_{HX}^2+\left(1-3\psi^2\right)\lambda_h\lambda_X\right)\omega^2\right) \\
&+ 4\left(\frac{M_J}{v_S}\right)^2\left[\left(-1+\psi^2\right)\lambda_{HS}^2-2\lambda_{HS}\lambda_{HX}\omega\left(2\psi\sqrt{1-\psi^2}-3\omega+3\psi^2\omega\right)\right. \\
&+ \left.\left.\left.\lambda_{HX}^2\omega^2\left(12\psi\sqrt{1-\psi^2}\omega+3\omega^2-\psi^2\left(4+3\omega^2\right)\right)\right]\right\]
\end{aligned} \tag{B.17}$$

Finally, we show the expressions for the couplings that lead to the Higgs invisible decays $H \longrightarrow 2\zeta_1$, $H \longrightarrow 2\zeta_2$ and $H \longrightarrow \zeta_1\zeta_2$. These formuli show that the contributions from the new fields $\zeta_{1,2}$ to the invisible Higgs decay are heavily supressed, since they are proportional to $\left(\frac{M_J}{v_s}\right)^2$. On top of that, observe that these expressions also depend on $\lambda_{HX}$ and $\lambda_{SH}$, couplings that have been taken to be $\ll 1$.

$$\begin{aligned}\lambda_{215} = & -24\left(\frac{M_J}{v_s}\right)^2 \frac{v_h\,\psi\,\omega^2}{(1+9\omega^2)^2\left\{A^2\left(-1+\psi^2\right)+4A\psi^2\lambda_X\omega^2+4\psi^2\lambda_X^2\omega^4\right\}} \\ & \Big[\lambda_{HS}\left\{3A\sqrt{1-\psi^2}+2\psi\lambda_X\omega-12\psi\lambda_X\omega^3\right\} \\ & + \lambda_{HX}\left\{6\psi\lambda_X\omega^3+A\left(6\psi\omega+\sqrt{1-\psi^2}\left(1-6\omega^2\right)\right)\right\}\Big] \end{aligned} \tag{B.18}$$

$$\begin{aligned}\lambda_{115} = & -24\left(\frac{M_J}{v_s}\right)^2 \frac{v_h\,\psi\,\omega}{(1+9\omega^2)^2\left\{A^2\left(-1+\psi^2\right)+4A\psi^2\lambda_X\omega^2+4\psi^2\lambda_X^2\omega^4\right\}} \\ & \Big[\lambda_{HS}\left\{A\sqrt{1-\psi^2}-10\psi\lambda_X\omega^3\right\} \\ & + \lambda_{HX}\left\{2\psi\ \lambda_X\omega^3+A\omega\left(2\psi-5\sqrt{1-\psi^2}\omega\right)\right\}\Big] \end{aligned} \tag{B.19}$$

$$\begin{aligned}\lambda_{225} = & -72\left(\frac{M_J}{v_S}\right)^2 \frac{v_h\,\psi\,\omega^3}{(1+9\omega^2)^2\left\{A^2\left(-1+\psi^2\right)+4A\psi^2\lambda_X\omega^2+4\psi^2\lambda_X^2\omega^4\right\}} \\ & \Big[2\psi\lambda_X\omega\left\{3\lambda_{HX}\omega^2+\lambda_{HS}\left(2+3\omega^2\right)\right\} \\ & + A\left\{3\sqrt{1-\psi^2}\lambda_{HS}+\lambda_{HX}\left(6\psi\omega+\sqrt{1-\psi^2}\left(2+3\omega^2\right)\right)\right\}\Big] \end{aligned} \tag{B.20}$$

## Acknowledgments

This work was supported by the Spanish MINECO under grants FPA2014-58183-P, and MULTIDARK CSD2009-00064 (Consolider-Ingenio 2010 Programme); by Generalitat Valenciana grant PROMETEOII/2014/084, and Centro de Excelencia Severo Ochoa SEV-2014-0398. R. A. L. acknowledges the support of the Juan de la Cierva contract JCI-2012-12901 (MINECO) and the Spanish MESS via the *Servicio Público de Empleo Estatal*. N. R. was funded by becas de postdoctorado en el extranjero Conicyt/Becas Chile 74150028. N. R. also wants to thank P. Sánchez for her constant support and all the members at the AHEP group for the hospitality. F.G.C. acknowledges the financial support from CONACYT, CONACYT-SNI and PAPIIT IN111115.

[1] S. Weinberg, *A Model of Leptons*, *Phys. Rev. Lett.* **19** (1967) 1264–1266.

[2] P. W. Higgs, *Broken Symmetries and the Masses of Gauge Bosons*, *Phys. Rev. Lett.* **13** (1964) 508–509.

[3] U A 1 collaboration, G. Arnison et al., *Experimental Observation of Isolated Large Transverse Energy Electrons with Associated Missing Energy at s**(1/2) = 540-GeV*, *Phys. Lett.* **122B** (1983) 103–116.

[4] U A 2 collaboration, P. Bagnaia et al., *Evidence for Z0 —¿ e+ e- at the CERN anti-p p Collider*, *Phys. Lett.* **B129** (1983) 130–140.

[5] ATLAS collaboration, G. Aad et al., *Observation of a new particle in the search for the Standard Model Higgs boson with the ATLAS detector at the LHC*, *Phys. Lett.* **B716** (2012) 1–29, [1207.7214].

[6] CMS collaboration, S. Chatrchyan et al., *Observation of a new boson at a mass of 125 GeV with the CMS experiment at the LHC*, *Phys. Lett.* **B716** (2012) 30–61, [1207.7235].

[7] J. H. Oort, *The force exerted by the stellar system in the direction perpendicular to the galactic plane and some related problems*, *bain* **6** (Aug., 1932) 249.

[8] V. C. Rubin, N. Thonnard and W. K. Ford, Jr., *Rotational properties of 21 SC galaxies with a large range of luminosities and radii, from NGC 4605 /R = 4kpc/ to UGC 2885 /R = 122 kpc/*, *Astrophys. J.* **238** (1980) 471.

[9] Planck collaboration, P. A. R. Ade et al., *Planck 2015 results. XIII. Cosmological parameters*, *Astron. Astrophys.* **594** (2016) A13, [1502.01589].

[10] B. Pontecorvo, *Mesonium and anti-mesonium*, *Sov. Phys. JETP* **6** (1957) 429.

[11] Z. Maki, M. Nakagawa and S. Sakata, *Remarks on the unified model of elementary particles*, *Prog. Theor. Phys.* **28** (1962) 870–880.

[12] SNO collaboration, Q. R. Ahmad et al., *Measurement of the rate of $\nu_e + d \to p + p + e^-$ interactions produced by $^8B$ solar neutrinos at the Sudbury Neutrino Observatory*, *Phys. Rev. Lett.* **87** (2001) 071301, [nucl-ex/0106015].

[13] Super-Kamiokande collaboration, Y. Fukuda et al., *Measurement of a small atmospheric muon-neutrino / electron-neutrino ratio*, *Phys. Lett.* **B433** (1998) 9–18, [hep-ex/9803006].

[14] M. Lattanzi, R. A. Lineros and M. Taoso, *Connecting neutrino physics with dark matter*, *New J. Phys.* **16** (2014) 125012, [1406.0004].

[15] M. Hirsch, R. A. Lineros, S. Morisi, J. Palacio, N. Rojas and J. W. F. Valle, *WIMP dark matter as radiative neutrino mass messenger*, *JHEP* **10** (2013) 149, [1307.8134].

[16] Particle Data Group collaboration, C. Patrignani et al., *Review of Particle Physics*, *Chin. Phys.* **C40** (2016) 100001.

[17] I. Esteban, M. C. Gonzalez-Garcia, M. Maltoni, I. Martinez-Soler and T. Schwetz, *Updated fit to three neutrino mixing: exploring the accelerator-reactor complementarity*, *JHEP* **01** (2017) 087, [1611.01514].

[18] F. Capozzi, E. Lisi, A. Marrone, D. Montanino and A. Palazzo, *Neutrino masses and mixings: Status of known and unknown $3\nu$ parameters*, *Nucl. Phys.* **B908** (2016) 218–234, [1601.07777].

[19] D. V. Forero, M. Tortola and J. W. F. Valle, *Neutrino oscillations refitted*, *Phys. Rev.* **D90** (2014) 093006, [1405.7540].

[20] S. Weinberg, *Baryon and Lepton Nonconserving Processes*, *Phys. Rev. Lett.* **43** (1979) 1566–1570.

[21] P. Minkowski, *$\mu \to e\gamma$ at a Rate of One Out of $10^9$ Muon Decays?*, *Phys. Lett.* **B67** (1977) 421–428.

[22] R. N. Mohapatra and G. Senjanovic, *Neutrino Mass and Spontaneous Parity Violation*, *Phys. Rev. Lett.* **44** (1980) 912.

[23] J. Schechter and J. W. F. Valle, *Neutrino Masses in SU(2) x U(1) Theories*, *Phys. Rev.* **D22** (1980) 2227.

[24] R. N. Mohapatra and G. Senjanovic, *Neutrino Masses and Mixings in Gauge Models with Spontaneous Parity Violation*, *Phys. Rev.* **D23** (1981) 165.

[25] R. Foot, H. Lew, X. G. He and G. C. Joshi, *Seesaw Neutrino Masses Induced by a Triplet of Leptons*, *Z. Phys.* **C44** (1989) 441.

[26] Riazuddin, R. E. Marshak and R. N. Mohapatra, *Majorana Neutrinos and Low-energy Tests of Electroweak Models*, *Phys. Rev.* **D24** (1981) 1310–1317.

[27] I. Z. Rothstein, K. S. Babu and D. Seckel, *Planck scale symmetry breaking and majoron physics*, *Nucl. Phys.* **B403** (1993) 725–748, [hep-ph/9301213].

[28] M. S. Boucenna, R. A. Lineros and J. W. F. Valle, *Planck-scale effects on WIMP dark matter*, *Front.in Phys.* **1** (2013) 34, [1204.2576].

[29] V. Berezinsky and J. W. F. Valle, *The KeV majoron as a dark matter particle*, *Phys. Lett.* **B318**

(1993) 360–366, [hep-ph/9309214].

[30] A. Aranda and F. J. de Anda, *Electroweak scale neutrinos and decaying dark matter*, *Phys. Lett.* **B683** (2010) 183–185, [0909.2667].

[31] M. Lattanzi and J. W. F. Valle, *Decaying warm dark matter and neutrino masses*, *Phys. Rev. Lett.* **99** (2007) 121301, [0705.2406].

[32] C. Garcia-Cely and J. Heeck, *Neutrino Lines from Majoron Dark Matter*, 1701.07209.

[33] R. N. Mohapatra, *Mechanism for Understanding Small Neutrino Mass in Superstring Theories*, *Phys. Rev. Lett.* **56** (1986) 561–563.

[34] R. N. Mohapatra and J. W. F. Valle, *Neutrino Mass and Baryon Number Nonconservation in Superstring Models*, *Phys. Rev.* **D34** (1986) 1642.

[35] S. M. Barr, *A Different seesaw formula for neutrino masses*, *Phys. Rev. Lett.* **92** (2004) 101601, [hep-ph/0309152].

[36] A. Abada and M. Lucente, *Looking for the minimal inverse seesaw realisation*, *Nucl. Phys.* **B885** (2014) 651–678, [1401.1507].

[37] P. Humbert, M. Lindner and J. Smirnov, *The Inverse Seesaw in Conformal Electro-Weak Symmetry Breaking and Phenomenological Consequences*, *JHEP* **06** (2015) 035, [1503.03066].

[38] A. G. Dias, C. A. de S. Pires, P. S. Rodrigues da Silva and A. Sampieri, *A Simple Realization of the Inverse Seesaw Mechanism*, *Phys. Rev.* **D86** (2012) 035007, [1206.2590].

[39] P. Humbert, M. Lindner, S. Patra and J. Smirnov, *Lepton Number Violation within the Conformal Inverse Seesaw*, *JHEP* **09** (2015) 064, [1505.07453].

[40] S. C. Chuliá, R. Srivastava and J. W. F. Valle, *CP violation from flavor symmetry in a lepton quarticity dark matter model*, *Phys. Lett.* **B761** (2016) 431–436, [1606.06904].

[41] P.-H. Gu, E. Ma and U. Sarkar, *Pseudo-Majoron as Dark Matter*, *Phys. Lett.* **B690** (2010) 145–148, [1004.1919].

[42] C. Q. Geng and J. N. Ng, *A Minimal Spontaneous CP Violation Model With Small Neutrino Mass and SU(2) X U(1) X Z(3) Symmetry*, *Phys. Lett.* **B211** (1988) 111–116.

[43] E. K. Akhmedov, Z. G. Berezhiani, R. N. Mohapatra and G. Senjanovic, *Planck scale effects on the majoron*, *Phys. Lett.* **B299** (1993) 90–93, [hep-ph/9209285].

[44] M. Cirelli, E. Moulin, P. Panci, P. D. Serpico and A. Viana, *Gamma ray constraints on Decaying Dark Matter*, *Phys. Rev.* **D86** (2012) 083506, [1205.5283].

[45] J. Schechter and J. W. F. Valle, *Neutrino Decay and Spontaneous Violation of Lepton Number*, *Phys. Rev.* **D25** (1982) 774.

[46] L. J. Hall, K. Jedamzik, J. March-Russell and S. M. West, *Freeze-In Production of FIMP Dark Matter*, *JHEP* **03** (2010) 080, [0911.1120].

[47] P. Gondolo and G. Gelmini, *Cosmic abundances of stable particles: Improved analysis*, *Nucl. Phys.* **B360** (1991) 145–179.

[48] CMS collaboration, S. Chatrchyan et al., *Search for invisible decays of Higgs bosons in the vector boson fusion and associated ZH production modes*, *Eur. Phys. J.* **C74** (2014) 2980, [1404.1344].

[49] S. Baek, P. Ko and W.-I. Park, *Invisible Higgs Decay Width vs. Dark Matter Direct Detection Cross Section in Higgs Portal Dark Matter Models*, *Phys. Rev.* **D90** (2014) 055014, [1405.3530].